Yielding Limit State of Tee Stems in Flexural Compression

C.J. EARLS and L.E. VOLLE

Steel tee beams are typically either fabricated from plate, as built-up members, or obtained from cutting a rolled I-shaped member longitudinally along its centroidal axis; the latter case being the more frequently used in practice. In either case, the general treatment of tee members is somewhat ambiguous (Salmon and Johnson, 1996) within AISC specifications (AISC, 2000, 1989). It appears that consideration of tee beams as an extreme example of mono-symmetry in an I-shaped cross section has some precedent (Salmon and Johnson, 1996; Galambos, 2001), and is useful in a number of design applications. However, in terms of ductility and rotation capacity, within a flexural context, such an approach may be problematic since the nature of the plate boundary conditions present in the webs of mono-symmetric I-shaped cross sections differs substantially from that of outstanding tee stems in compression (in other words, the former being a stiffened element and the latter being unstiffened). Currently, AISC makes no attempt to quantify compactness limits for the case of tee stems in compression. The current paper presents research findings that support the notion that WT stems in compression may be considered compact; subject to certain limitations.

BASIS FOR CURRENT CROSS-SECTIONAL COMPACTNESS LIMITS FOR UNSTIFFENED ELEMENTS

The goal of the AISC compactness criteria promulgated in Table B5.1 of the *Load Resistance Factor Design Specification for Structural Steel Buildings* (AISC, 2000), hereafter referred to as the AISC *LRFD Specification*, is to identify plate slenderness limits, λ_p, for cross-sectional plate components such that satisfaction of said limits will result in an overall flexural cross section able to accommodate sufficient plastic hinge rotation to support system-wide moment redistribution as required for the development of a global collapse mechanism. In pursuit of this condition, and as a general guiding principle, compactness limits have historically been formulated to loosely accommodate strains approaching strain hardening values within an individual plate component prior to the attenuation of post-buckling strength due to effects of material nonlinearity.

Prior to any subsequent discussion of tee stem compactness, it is useful to consider the basis by which the AISC *LRFD Specification* addresses plate compactness within the context of another type of unstiffened element; flanges in I-shaped cross sections under uniform flexural compression. In this latter case, the question of how to address the uncertainty with regard to the nature of rotational edge restraint provided at the plate boundary associated with the flange-web junction is addressed through consideration of the work carried out by Haaijer and Thurlimann (1958). Haaijer and Thurlimann discovered that unstiffened plates exhibit the onset of strain hardening at slenderness values, λ_c, of approximately 0.46 irrespective of whether the supported edge is fixed or pinned. In this discussion, slenderness is defined as

$$\lambda_c = \sqrt{\frac{F_y}{F_{cr}}} \tag{1}$$

where classical elastic plate buckling theory provides that

$$F_{cr} = k\frac{\pi^2 E}{12\left(1-\nu^2\right)\left(\frac{b}{t}\right)^2} \tag{2}$$

in which E and ν are the usual elastic material constants and b and t are the plate width and thickness quantities, respectively. The term k is the plate buckling coefficient which depends on the plate aspect ratio, edge support conditions, and stress distribution along the loaded edge. In the case of an I-shaped cross-sectional flange, the two extremes that k can assume are: 0.425 for the case of a supported edge that

C.J. Earls is associate professor and William Kepler Whiteford Faculty Fellow, department of civil and environmental engineering, University of Pittsburgh, Pittsburgh, PA.

L.E. Volle is civil associate, Michael Baker Jr., Inc., Moon Township, PA.

is pinned; and 1.277 for the case of a rotationally-fixed supported edge. If we set Equation 2 equal to the yield stress, F_y, and solve for the width-to-thickness ratio, *b/t*, we obtain Equation 3.

$$\frac{b}{t} = 162\sqrt{\frac{k}{F_y}} \tag{3}$$

As mentioned previously, Haaijer and Thurlimann have observed that unstiffened plate components under the action of a uniform edge compression achieve strain hardening response at slenderness values, λ_c, of 0.46 and thus we may use Equation 3 to identify a plate slenderness limit for the attainment of strain hardening response as

$$\frac{b}{t} = 162\lambda_c\sqrt{\frac{k}{F_y}} = 74.5\sqrt{\frac{k}{F_y}} \tag{4}$$

The only question remaining is what value to assume for the plate buckling coefficient, *k*. It has been standard practice for AISC (AISC, 2000) to employ elastic plate buckling coefficients as a guide in the development of actual design specification equations and as such we may consider that the two extreme values for the present case of an I-section flange: 0.425 and 1.277 for the pinned and fixed cases, respectively, serve as reasonable bounds. If we, somewhat arbitrarily, consider one third of the difference between these two values and add this result to the smaller of the two we obtain a *k* of 0.71 which can be applied to Equation 4 so that we arrive at a limiting plate slenderness value for the onset of strain-hardening of

$$\frac{b}{t} = \frac{63}{\sqrt{F_y}} \approx \frac{65}{\sqrt{F_y}} = 0.38\sqrt{\frac{E}{F_y}} \tag{5}$$

It is noted that Equation 5 represents the current compactness limit, λ_p, presented in the AISC *LRFD Specification* in Table B5.1 for the case of an I-section flange under the action of uniform flexural compression.

We may employ a similar approach to the foregoing when developing a compactness limit for the case of a tee stem subjected to flexural compression; if we assume that Haaijer and Thurlimann's results concerning the invariance of λ_c with the degree of rotational restraint present at the supported edge in a uniformly compressed unstiffened element holds for the case of non-uniform compression. Non-uniform compression stresses would be observed along the loaded plate edge in a tee stem subjected to flexural compression (as depicted in Figure 1). While Haaijer and Thurlimann did consider the case of non-uniform compressive stresses within a plate component, their investigation centered on the case of a stiffened element; as is consistent with the web of an I-shaped cross section; a condition quite different from a tee stem. Proceeding with the assumption that the invariance in λ_c holds for the unstiffened case of a tee stem, we may reuse Equation 4 as the basic requirement for the attainment of strain hardening in a non-uniformly compressed plate component. In fact, current understanding would characterize this as a conservative approach to the problem since existing analytical solutions predict that a linearly varying stress field acting along a loaded edge is a less critical condition as compared with that of the uniformly distributed case. What is now left to do in the development of a compactness limit for tee stems in non-uniform flexural compression is to identify a suitable plate buckling coefficient, *k*. Guidance on the selection of an appropriate *k* value is obtained using the tabulated cases presented by Galambos (1998). We may conservatively assume that the full depth of the tee stem experiences compressive stress (in other words, we assume that the neutral axis is at the flange-web junction and no portion of the WT stem experiences tension). Two extreme values for *k* in this case may then be identified: 0.57 for a pinned supporting edge and 1.61 for a rotationally-restrained supporting edge. Proceeding as was done for the case of an I-shaped beam flange, we may add one third of the difference between the *k* values of these two extremes to the smaller of the two to arrive at *k* = 0.92. We may then employ this value in Equation 4 to arrive at a limiting plate slenderness value of

$$\frac{b}{t} = \frac{71}{\sqrt{F_y}} \approx 0.42\sqrt{\frac{E}{F_y}} \tag{6}$$

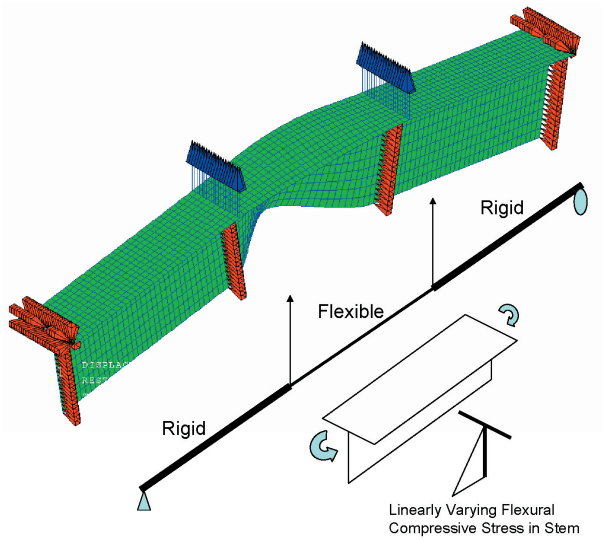

Fig. 1. Depiction of FE mesh and schematic of loading and stress condition.

The limits obtained from Equation 6 can now be compared with results obtained from a finite element parametric study considering tee beams having various parametric combinations of: flange width-to-cross-sectional depth ratio, b_f/d; unbraced length-to-cross-sectional depth ratio, L_b/d; ratio of stem depth-to-stem thickness, h/t_w; and the ratio of flange width-to-flange thickness, $b_f/2t_f$.

SCOPE

The current research focuses on tee beams subjected to a constant moment loading resulting in tee stem flexural compression with end conditions that are fixed against: out-of-plane translation, twisting, and warping (see Figure 1). The nonlinear finite element method is the vehicle by which the current research is carried out. A description of the modeling techniques employed is discussed in the sequel, but it is pointed out here that these same techniques have been experimentally verified for the cases of: minor principal axis flexure of single angle beams (Earls and Galambos, 1997), geometric axis flexure of single angle beams (Earls, 2001), major axis flexure of I-shaped beams (Thomas and Earls, 2003; Greco and Earls, 2003), and minor axis flexure of I-shaped beams (Aktas and Earls, 2004). Based on the favorable results from the foregoing validation studies carried out on closely related cases, the modeling strategies used herein are thought to be appropriate for the current focus of tee beam compactness.

The precise ranges within the parametric combinations treated in the present study are given as

$$0.6 \le \frac{b_f}{d} \le 2.0$$

$$1.8 \le \frac{L_{pd}}{d} \le 12.6$$

$$9.2 \le \frac{b_f}{2t_f} \le 12.9$$

$$6.7 \le \frac{h}{t_w} \le 16.5$$

FINITE ELEMENT MODELING TECHNIQUES

Background

The commercial multipurpose finite element software package ABAQUS version 5.8-22 is employed in this research. All modeling reported herein considers both nonlinear geometric and material influences. The incremental solution strategy chosen for this work is the modified Riks-Wempner method (ABAQUS, 2003) since this technique permits limit points on the equilibrium path to be negotiated. The ability to accurately negotiate such limit points is a prerequisite for any compactness study since unloading response is at the heart of the currently accepted measure for flexural ductility: rotation capacity, R. The definition for rotation capacity adopted in the present discussion is that presented by ASCE (1971)

$$R = (\theta_u / \theta_p) - 1 \qquad (7)$$

where

θ_u = rotation when the moment capacity drops below M_p on the unloading branch of the M-θ plot

θ_p = theoretical rotation at which the full plastic capacity is achieved based on elastic beam stiffness

This ductility response measure is described graphically in Figure 2 wherein θ_1 corresponds to θ_p, and θ_2 corresponds to θ_u in the ASCE definition. It is currently assumed that $R = 3$ is an adequate level of structural ductility for the nonseismic design of steel building components (AISC, 2000) and thus current compactness provisions are formulated with this measure in mind.

Material nonlinearity is modeled using ABAQUS' standard metal plasticity material model which is based on an incremental plasticity formulation employing associated flow assumptions in conjunction with a von Mises failure surface whose evolution in stress-space is governed by a simple isotropic hardening rule. The initial failure surface bounds of the virgin material state is defined by the analyst through the use of uniaxial true stress versus incremental logarithmic strain data that is imported into ABAQUS through input cards. In the present work, Grade 50 mild steel is considered;

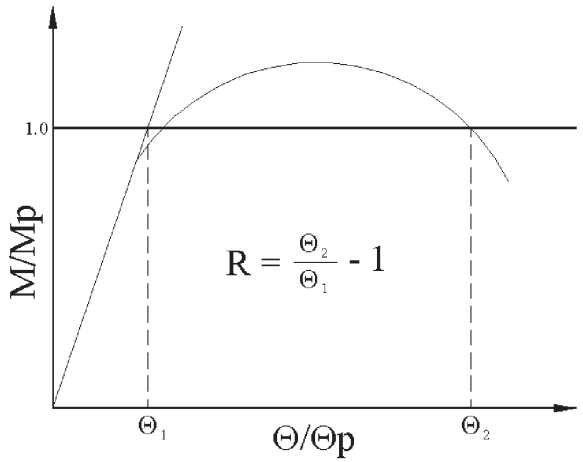

Fig. 2. Definition of rotation capacity.

Figure 3 displays a schematic representation of the uniaxial material response that is consistent with what is used in the present work. ABAQUS uses the uniaxial material response data stored in the input cards to develop a three-dimensional failure surface (in other words, a cylindrical surface centered on a generator corresponding to a purely hydrostatic loading condition) in principle stress space whose interior defines the range of purely elastic material response.

Figure 1 depicts the finite element mesh of a typical tee beam model used in the current study. The mesh consists of shell finite elements positioned so as to coincide with the middle surfaces of the cross-sectional plate components. ABAQUS S9R5 shell finite elements are used throughout this study since their performance within the context of compactness research on similar cases to the present one have been well documented (Earls and Galambos, 1997; Earls, 2001). The S9R5 shell finite element is a nine-noded quadratic element having five degrees of freedom per node (in other words, the out-of-plane "drilling" degree of freedom is not included in the element formulation) that employs reduced integration to control unwanted and spurious locking behaviors. While it is that the S9R5 is shear deformable in the spirit of Mindlin-Reissner plate theory (in other words, it accommodates explicit consideration of nodal rotations as a degree of freedom—and not as a partial derivative of the displacement field), it is nonetheless effective in modeling thin-shell response due to the imposition of Kirchhoff plate bending assumptions at discrete points on the Gauss surface of the shell elements by way of a penalty method.

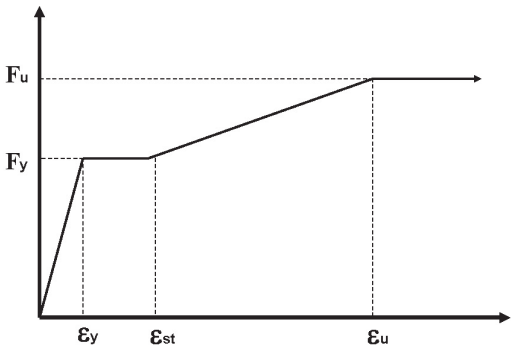

Material	F_y	F_u/F_y	$\varepsilon_{st}/\varepsilon_y$	$\varepsilon_u/\varepsilon_y$
Steel	50 ksi	1.6	5.5	45.0

Fig. 3. Uniaxial constitutive model considered.

Modeling Overview

A constant moment condition is imposed on all tee beams considered as part of this study since this loading case represents the most severe flexural condition and as such is the case explicitly treated in the development of design specification equations for nominal moment capacity. The constant moment loading is achieved in the current finite element models by applying concentrated forces perpendicular to the beam longitudinal axis at two points on a simply-supported span as depicted in Figure 1. The beam is separated into three segments, each having a length of L_{pd} as specified in AISC *LRFD Specification* Section F1.3 (AISC, 2000); with the two end segments being modeled with exaggerated plate thickness and an elastic modulus ten times greater than that of steel (in other words, 300,000 ksi) to approximate a rigid condition. The concentrated forces are applied to the cross-sectional shear center of the beams. Restraint against out-of-plane translation is enforced at all nodes along the interfaces between the rigid and flexible segments. As a result of this out-of-plane restraint being provided all along the tee stem height, torsional restraint is also effectively provided at the bracing locations. Furthermore, as a result of the rigid end sections, these same locations also experience a complete restraint of warping deformations.

Due to the fact that unloading in adequately braced tee beams experiencing a fully-yielded condition is most frequently triggered by local buckling of the tee stem in compression, the present work may be characterized as an inelastic buckling study. As with any type of buckling study involving the incremental nonlinear finite element method (in other words, cases where true bifurcation response dominates within the case of perfect geometry), an initial seed imperfection is required within the mesh so as to guard against the tendency of most finite element solver routines to remain on the primary equilibrium branch even after a bifurcation point has been passed. While in an elastic analysis we can say for certain that remaining on the primary equilibrium path after bifurcation would result in the solution following an unstable equilibrium branch, the same cannot be said, with utter certainty, in an inelastic buckling analysis (Bazant and Cedolin, 1991; Teh and Clark, 1999). However, in a practical sense for structural engineering work, it is most likely a reasonable assumption to consider this primary path as unstable after bifurcation; even within the inelastic material response regime. In any case, a useful modeling strategy for the study of inelastic buckling problems with the incremental nonlinear finite element technique is to seed the previously perfect mesh with an imperfection displacement field of sufficient magnitude to annihilate the bifurcation quality of the problem and produce an equivalent load-displacement problem in its place that asymptotically approaches the load level at bifurcation (Timoshenko and Gere, 1961). To this end, a linearized eigenvalue buckling analysis (ABAQUS, 2003) is

Table 1. Finite Element Results at Small Span-to-Depth Ratios

$\frac{b_f}{d}$	$\frac{L_{pd}}{d}$	$\frac{b_f}{2t_f}$	$\frac{h}{t_w}$	$\frac{M_u}{M_p}$	R
0.6	2.1	9.2	13.5	0.75	-
0.6	2.0	9.2	11.3	0.78	-
0.6	1.9	9.2	9.7	0.85	-
0.6	1.9	9.2	8.5	0.95	-
0.6	1.9	9.2	7.5	1.05	11.6
0.6	1.8	9.2	6.8	1.12	17.1
0.8	3.5	9.2	13.4	0.78	-
0.8	3.3	9.2	11.2	0.79	-
0.8	3.1	9.2	9.6	0.80	-
0.8	3.0	9.2	8.4	0.84	-
0.8	2.9	9.2	7.4	0.90	-
0.8	2.8	9.2	6.7	1.00	-
1.0	5.2	9.2	16.5	0.90	-
1.0	4.9	9.2	13.2	0.90	-
1.0	4.8	9.2	12.0	0.90	-
1.0	4.7	9.2	11.0	0.89	-
1.0	4.6	9.2	10.2	0.88	-

performed on each tee beam parametric combination considered within the study so as to obtain approximations to the first ten elastic buckling modes of the given tee beam. For each parametric combination, each of the ten modes are examined so as to identify the mode possessing a pronounced stem local buckling feature. This mode is then scaled by a factor of L_b/1000 and employed as a seed imperfection on the perfect mesh used to carry out a fully non-linear incremental finite element analysis.

RESULTS

Finite element studies of 50 different tee beam parametric combinations are carried out as part of the present study. Despite the fact that the focus of the work is on tee beam compactness when the stem is in compression, and the flanges are in tension, the majority of the parametric combinations considered herein are carried out using compact flanges as outlined in Table B5.1 of the AISC *LRFD Specification*

$$\lambda_p = 0.38\sqrt{\frac{E}{F_y}} = 0.38\sqrt{\frac{29{,}000\,\text{ksi}}{50\,\text{ksi}}} = 9.15 \qquad (8)$$

As can be seen from Equation 8, the flanges are proportioned to be right at the limit of compactness. This approach is taken since it was not initially clear what role end rotational restraint, as provided by the flange at the flange-web junction, might have on the manifestation of local buckling in the compressed stem. The effect of this edge restraint turned out to be of little importance as is demonstrated later in the present paper.

Discussion of Results

Table 1 presents early results obtained from the present study that highlight an interesting detail regarding limits on just how short one can make a tee beam before shear effects erode the ability of a theoretical plastic hinge to evolve. In the table we see that many of the parametric combinations listed involve very stocky cross-sectional plate combinations that ought to easily produce a cross section capable of developing a ductile response. However, what was observed was that while the moment-rotation results of the tee beams was ductile in the sense that gradual unloading from the ultimate moment value occurred, the ultimate moment rarely achieved M_p. The cause of this observed behavior is easily explained

Table 2. Finite Element Results with Acceptable Span-to-Depth Ratios					
$\frac{b_f}{d}$	$\frac{L_{pd}}{d}$	$\frac{b_f}{2t_f}$	$\frac{h}{t_w}$	$\frac{M_u}{M_p}$	R
1.2	6.7	9.2	14.5	0.98	-
1.2	6.6	9.2	13.8	1.01	1.33
1.2	6.5	9.2	13.4	1.03	1.86
1.2	6.5	9.2	13.2	1.03	3.50
1.2	6.2	9.2	10.9	1.16	5.26
1.4	8.1	9.2	12.9	1.01	1.64
1.4	8.0	9.2	11.8	1.06	3.07
1.4	7.9	9.2	11.3	1.12	4.55
1.4	7.7	9.2	10.0	1.17	8.02
1.6	9.5	9.2	10.9	1.05	3.15
1.6	8.8	9.2	10.7	1.06	3.63
1.6	9.3	9.2	9.8	1.11	5.69
1.6	9.0	9.2	8.5	1.25	11.23
1.8	11.1	9.2	10.5	1.03	2.89
1.8	11.0	9.2	10.4	1.03	3.19
1.8	10.4	9.2	9.7	1.07	4.34
1.8	10.8	9.2	9.0	1.13	6.58
1.8	10.7	9.2	8.4	1.20	9.26
1.8	10.5	9.2	7.9	1.24	12.09
2.0	12.6	9.2	10.0	1.01	3.12
2.0	12.5	9.2	9.6	1.03	3.89
2.0	12.4	9.2	8.9	1.09	5.77
2.0	12.3	9.2	8.3	1.08	6.30

by an examination of the plot of von Mises stresses occurring within the finite element mesh (an example is presented in Figure 4). The von Mises stress contours indicate that the tee beams are most certainly fully yielded, however a significant portion of this yielding is due to shear effects in the very short beams, meaning, at very short beam unbraced lengths, the multiaxial state of stress at the given material points in the mesh is sufficient to activate yielding of the steel. The net result of this behavior is that due to the presence of high shear stresses, only small longitudinal stresses can be accommodated prior to the initiation of yielding at a given material point. A useful analogy to illustrate the net effect of this result might be that a designer specifies, and expects to receive, a Grade 50 steel beam and bases his/her calculations for M_p on a specified minimum yield stress of 50 ksi. However, the steel beam that shows up only has a yield stress of 36 ksi and hence it achieves an M_p, but unfortunately one that is much lower than expected. This type of effect (in other words, effective longitudinal yield stresses lower than expected due to the material's capacity being consumed by shear stress) is observed in the present finite element studies when the unbraced length-to-depth ratios are less than 6.5; and thus, most of the later finite element parametric studies

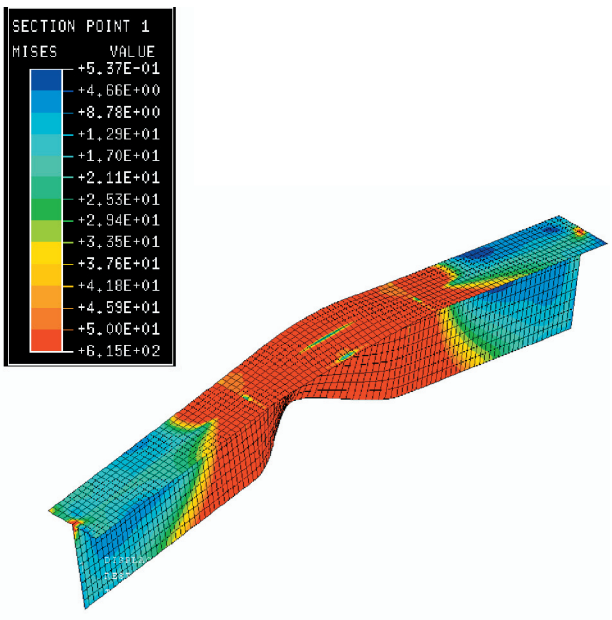

Fig. 4. Depiction of von Mises stresses in a tee at ultimate load.

Table 3. Finite Element Results with Flange Slenderness Set Equal to 1.2 (λ_p)					
$\frac{b_f}{d}$	$\frac{L_{pd}}{d}$	$\frac{b_f}{2t_f}$	$\frac{h}{t_w}$	$\frac{M_u}{M_p}$	R
1.2	6.2	11.0	13.2	1.05	1.81
1.4	7.6	11.0	11.9	1.07	5.62
1.6	9.1	11.0	11.1	1.07	3.70
1.8	10.7	11.0	10.5	1.05	3.18
2.0	12.3	11.0	10.2	1.03	3.07

Table 4. Finite Element Results with Flange Slenderness Set Equal to 1.4 (λ_p)					
$\frac{b_f}{d}$	$\frac{L_{pd}}{d}$	$\frac{b_f}{2t_f}$	$\frac{h}{t_w}$	$\frac{M_u}{M_p}$	R
1.2	6.0	12.9	13.4	0.91	-
1.4	9.4	12.9	12.0	1.05	2.92
1.6	8.8	12.9	11.2	1.08	3.87
1.8	10.35	12.9	10.7	1.05	3.39
2.0	11.9	12.9	10.3	1.04	3.26

are carried out using the following criterion:

$$\frac{L_{pd}}{d} \geq 6.5 \tag{9}$$

Since the models are constructed such that the flexible region of the tees are exactly L_{pd} in length, the bracing requirements outlined in Sections F1.2a and F1.3 of the AISC *LRFD Specification*, as required for the attainment of M_p with the ability to accommodate moment redistribution, are still satisfied.

Table 2 presents additional finite element results from models satisfying the above mentioned criterion regarding an acceptable unbraced length-to-depth ratio. From these results, it is observed that in order to satisfy the compactness requirement for a plastic hinge rotation capacity of three, the plate slenderness, h/t_w, of the compressed Grade 50 tee stem should be given as:

- For $b_f/d = 1.2$, then $\lambda_p \leq 13.1$
- For $b_f/d = 1.4$, then $\lambda_p \leq 11.8$
- For $b_f/d = 1.6$, then $\lambda_p \leq 10.9$
- For $b_f/d = 1.8$, then $\lambda_p \leq 10.4$
- For $b_f/d = 2.0$, then $\lambda_p \leq 10.0$

Based on the foregoing it is noticed that the data seem to indicate that the limiting plate slenderness of the tee stem, h/t_w, seems to be inversely related to b_f/d. However, as will be seen later in this paper, this effect is mostly like due to the fact that unbraced length is increasing as b_f/d grows (as can be seen in Table 2), and not due to any difference in edge restraint present at the tee stem flange-web junction (as might be implied by a variation in b_f/d).

The effects of WT edge restraint provided by the flange at the flange-web junction can be investigated through the consideration of the finite element results presented in Tables 3 and 4. These two tables contain tee stem response data obtained when flange slenderness grows, from $1.0\lambda_p$ to $1.2\lambda_p$ and then again to $1.4\lambda_p$, while all other parametric combina-

tions are held constant. Based on these results it appears that, for the case of WT cross sections whose b_f/d ratios lie between 1.4 and 2.0 [for example, the lighter rolled WT sections in the AISC *Load and Resistance Factor Design Manual of Steel Construction* (AISC, 2001)], the slenderness of the flange only slightly impacts the web stem compactness in flexural compression. Based on the results given in Tables 3 and 4, it seems very reasonable to ignore this effect in a practical sense and consider that within the b_f/d ratios mentioned, flange slenderness has essentially no impact up to $1.4\lambda_p$ for the flange (as presented in Equation 8).

Recommendations

Based on the results from the finite element studies presented in Tables 1 through 4, it appears that a conservative limiting plate slenderness for Grade 50 steel tee beams subjected to constant moment loading might be $h/t_w = 10$. It is noticed that this value agrees quite well with the conclusions of the discussion presented in the introductory portion of the current paper where it was pointed out that Equation 6 might be applicable to the problem at hand. Indeed, for the case of Grade 50 steel, Equation 6 would predict that an h/t_w ratio equal to 10 ought to be adequate for compactness. This last point is tempered by the requirement described in Equation 9. In addition, satisfaction of the bracing requirements outlined in Sections F1.2a and F1.3 of the AISC *LRFD Specification* (AISC, 2000) would also be required for achieving moment redistribution.

It is pointed out that tee beams frequently have shape factors (defined as the ratio of plastic to elastic section moduli) that are quite large (for example, approaching two, or more, in some cases). Within a load and resistance factor design context, employing the load case combinations from ASCE 7 (ASCE, 2002), it may arise that designs predicated on tee beams developing full theoretical moment capacities, M_p, may suffer from yielding under service loading conditions. This is a condition that the designer must be aware of in any attempt to rely on the ability of a given tee beam to attain M_p and subsequently maintain this load level so as to redistribute moments in a larger structural system.

CONCLUSIONS

It appears from the results presented herein that it is possible to attain the theoretical plastic moment capacity, M_p, when a tee beam is bent under the action of a constant moment loading such that its stem experiences flexural compression. Furthermore, it appears possible to identify limiting plate slenderness ratios for the tee stem, h/t_w, such that compact cross-sectional behavior ensues. Both of these conclusions are predicated on the tee beam having a sufficiently large unbraced-length-to-depth ratio, L_{pd}/d, such that premature yielding within the cross section does not occur as a result of large shear stresses developing. Furthermore, it is pointed out that within an LRFD design context, the large shape factors commonly exhibited by tee beams may result in a condition where yielding may occur under service loads and hence must be a consideration of the designer who may wish to use tee beams in designs requiring plastic moment redistribution.

NOTATION

b_f	Flange width
d	Overall cross-sectional depth of tee beam
t	Plate thickness
t_f	Flange thickness
t_w	Tee stem thickness
h	Overall depth minus the flange cross-sectional depth: $(d - t_f)$
L_b	Unbraced length of tee beam
L_{pd}	Maximum unbraced length permitted for use with moment redistribution
E	Modulus of elasticity
ν	Poisson's ratio
F_{cr}	Plate buckling stress
F_y, σ_y	Steel yield stress (true stress measure)
F_u, σ_u	Steel ultimate strength (true stress measure)
k	Plate buckling coefficient depending on plate aspect ratio, edge support conditions, and stress distribution along the loaded edge
ε_y	Steel strain at yield (logarithmic strain measure)
ε_{st}	Steel strain at the onset of strain-hardening (logarithmic strain measure)
ε_b	Intermediate strain-hardening strain (logarithmic strain measure)
ε_u	Steel ultimate strain (logarithmic strain measure)
λ	Plate slenderness parameter quantified by width-to-thickness ratio
λ_p	Compactness limit for plate cross-sectional plate slenderness needed for moment redistribution
θ_p	Cross-sectional rotation resulting in the attainment of the theoretical plastic moment
M_y	Moment causing the extreme cross-sectional fiber to yield
M_p	Full plastic capacity of cross section
M_u	Ultimate moment capacity
P	Concentrated force
R_y	Radius of gyration about the minor principal centroidal axis

REFERENCES

ABAQUS (2003), *ABAQUS Theory Manual*, Hibbitt, Karlsson & Sorensen, Inc., Pawtucket, RI.

AISC (1989), *Specification for Structural Steel Buildings—Allowable Stress Design and Plastic Design,* June 1, 1989, American Institute of Steel Construction, Inc., Chicago, IL.

AISC (2000), *Load and Resistance Factor Design Specification for Structural Steel Buildings*, December 27, 1999, American Institute of Steel Construction, Inc., Chicago, IL.

AISC (2001), *Load and Resistance Factor Design Manual of Steel Construction*, 3rd Ed., American Institute of Steel Construction, Inc., Chicago, IL.

Aktas, M. and Earls, C.J. (2004), "Ductility of I-Shaped Beams in Minor Axis Flexure," *Report No. CE/ST 27*, Department of Civil and Environmental Engineering, University of Pittsburgh, Pittsburgh, PA.

ASCE (1971), *Plastic Design in Steel, A Guide and Commentary*, American Society of Civil Engineers, New York, NY, p. 80.

ASCE (2002), *Minimum Design Loads for Buildings and Other Structures*, ASCE 7-02, American Society of Civil Engineers, Reston, VA.

Bazant, Z.P. and Cedolin, L. (1991), *Stability of Structures: Elastic, Inelastic, Fracture, and Damage Theories*, Oxford University Press, New York, NY.

Earls, C.J. (2001), "Single Angle Geometric Axis Flexure, Part I: Background and Model Verification," *Journal of Constructional Steel Research*, Elsevier Science Ltd., Great Britain, Vol. 57, pp. 603-622.

Earls, C.J. and Galambos, T.V. (1997), "Design Recommendations for Single Angle Flexural Members," *Journal of Constructional Steel Research*, Elsevier Science Ltd., Great Britain, Vol. 43, Issue 1-3, July–September, pp. 65-85.

Galambos, T.V., ed. (1998), *Guide to Stability Design Criteria for Metal Structures*, 5th Ed., John Wiley & Sons, Inc., New York, NY.

Galambos, T.V. (2001), "Strength of Singly Symmetric I-Shaped Beam-Columns," *Engineering Journal*, American Institute of Steel Construction, Inc., Vol. 38, No. 2, Second Quarter, Chicago, IL, pp. 65-77.

Greco, N. and Earls, C.J. (2003), "Structural Ductility in Hybrid High Performance Steel Beams," *Journal of Structural Engineering*, Vol. 129, No. 12, American Society of Civil Engineers, Reston, VA.

Haaijer, G. and Thurlimann, B. (1958), "On Inelastic Buckling in Steel," *Journal of the Engineering Mechanics Division*, Proceedings of the American Society of Civil Engineers, Paper 1581, EM 2, April, pp. 1581-1 to 1581-48.

Salmon, C.G. and Johnson, J.E. (1996), *Steel Structures, Design and Behavior,* 4th Ed., Harper Collins College Publishers, New York, NY.

Teh, L.H. and Clarke, M.J. (1999), "Tracing Secondary Equilibrium Paths of Elastic Framed Structures," *Journal of Engineering Mechanics*, Vol. 125, No. 12, American Society of Civil Engineers, Reston, VA, pp. 1358-1364.

Thomas, S. and Earls, C.J. (2003), "Cross Sectional Compactness and Bracing Requirements for HPS483W Girders," *Journal of Structural Engineering*, Vol. 129, No. 12, American Society of Civil Engineers, Reston, VA.

Timoshenko, S.P. and Gere, J.M. (1963), *Theory of Elastic Stability*, McGraw-Hill Book Company, New York, NY.